Hyperchaotic behaviours and controlling hyperchaos in an array of RCL-shunted Josephson junctions

Ri Ilmyong(李日明)[a)b)], Feng Yu-Ling(冯玉玲)[a)†], Yao Zhi-Hai(姚治海)[a)], and Fan Jian(范 健)[a)]

[a)] *Department of Physics, Science College, Changchun University of Science and Technology, Changchun* 130022, *China*
[b)] *Department of Physics, University of Science, Unjong Strict, Pyongyang, DPR Korea*

(Received 13 June 2011; revised manuscript received 13 July 2011)

This paper deals with dynamical behaviours in an array composed of two resistive-capacitive-inductive-shunted (RCL-shunted) Josephson junctions (RCLSJJs) and a shunted resistor. Numerical simulations show that periodic, chaotic and hyperchaotic states can coexist in this array. Moreover, a scheme for controlling hyperchaos in this array is presented by adjusting the external bias current. Numerical results confirm that this scheme can be effectively used to control hyperchaotic states in this array into stable periodic states, and different stable periodic states with different period numbers can be obtained by appropriately choosing the intensity of the external bias current.

Keywords: hyperchaos, controlling hyperchaos, array of RCL-shunted Josephson junctions, Lyapunov exponent

PACS: 05.45.Pq, 74.50.+r **DOI:** 10.1088/1674-1056/20/12/120504

1. Introduction

With the rapid development of fabrication technology and superconducting materials, Josephson junctions have been extensively utilized, and high critical-current junctions are preferred in many applications.[1] In order to further study Josephson junctions with higher critical currents, the resistive-capacitive-inductive-shunted Josephson junction (RCLSJJ) model was proposed[2] based on previous investigations of the resistive-capacitive shunted Josephson junction (RCSJJ) model.[3] Moreover, the RCLSJJ model has avoided the shortcomings of the RCSJJ model and shown the agreement between the experimental and the numerical simulated I–V curves when the shunt of the junction contains an inductive component.[3,4] Following this, there have been some reports on chaos, chaos control and chaotic synchronization in RCLSJJs.[5−16] Recently, much attention has been paid to the dynamical characteristics of the Josephson junction array (JJA), since the output power of a single junction is extremely low (typically 10 nW) and higher output power values can be obtained by using JJAs. Chaos and nonlinearity in JJAs have been interesting subjects of research[17−22] since JJAs could be used as high precision voltage standards, high power coherent THz sources, a new-type inductor, etc.[23,24] Basler *et al.*[17] reported on the theory of phase locking in a small Josephson junction cell by using the resistively shunted junction (RSJ) model. Hassel *et al.*[18] studied self-synchronization in distributed Josephson junction arrays by using the RSJ model. Grib *et al.*[19] reported on the synchronization of overdamped RCSJJs shunted by a superconducting resonator. Bhagavatula *et al.*[20] numerically investigated spatiotemporal chaos in the JJA composed of RSJs. Chernikov and Schmidt[21] studied JJAs composed of RSJs. The dynamical equation set was approximated in their research. They found that when four or more units are globally coupled by a common resistance, the system exhibits adiabatic chaos. Zhou *et al.*[22] studied a JJA composed of RCSJJs. The dynamical equations were not approximated. Direct calculation results showed that phase locking and chaos coexist when there are three junctions in the JJA. Zhang and Shen,[25] and Feng *et al.*[26] completed controlling hyperchaos in erbium-doped fiber laser and degenerate optical parametric oscillators. In the present paper, we investigate chaos, hyperchaos and controlling hyperchaos in a JJA composed of RCLSJJs. The numerical results show that chaos and hyperchaos states can coexist in this array when it contains two RCLSJJs, no matter whether the original states of two RCLSJJs are chaotic. Moreover, we achieve the control of hyperchaos in this array by adjusting the intensity of the external bias current.

†Corresponding author. E-mail: fyl0819@yahoo.com.cn

© 2011 Chinese Physical Society and IOP Publishing Ltd

2. Array model and equation

In this section, we present an array model which consists of two RCLSJJs, a shunted resistance R and a direct current source. The circuit schematic diagram is shown in Fig. 1.

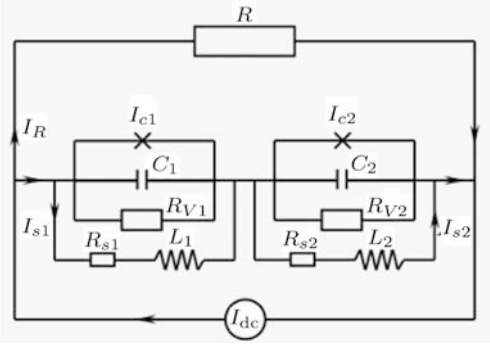


Fig. 1. Schematic diagram of the Josephson junction array.

If all the noise terms are neglected, its complete dynamical equations are as follows:

$$\frac{\hbar}{2e}\frac{\mathrm{d}\gamma_n}{\mathrm{d}t} = V_n, \tag{1}$$

$$C_n\frac{\mathrm{d}V_n}{\mathrm{d}t} + \frac{V_n}{R_{V_n}} + I_{\mathrm{cn}}(\sin\gamma_n) + I_{\mathrm{sn}} + I_R = I_{\mathrm{dc}}, \tag{2}$$

$$L_n\frac{\mathrm{d}I_{\mathrm{sn}}}{\mathrm{d}t} + I_{\mathrm{sn}}R_{\mathrm{sn}} = V_n, \tag{3}$$

$$I_R = \frac{1}{R}\sum_{n=1}^{2} V_n, \tag{4}$$

where subscripts $n = 1, 2$ denote the serial numbers of two RCLSJJs used in the array; C_n, I_{cn}, and γ_n are the junction capacitance, the junction critical current and the phase difference of the superconducting order parameters across the n-th RCLSJJ, respectively; V_n is the junction voltage; R_{Vn} is the nonlinear resistance; R_{sn} and L_n are, respectively, the shunt resistance and shunt inductance; I_{sn} is the shunt current flowing through R_{sn}; I_{dc} is the external bias dc current; $\hbar$ is the Planck constant; e is the electron charge.

For the convenience of numerical analysis, Eqs. (1)–(4) are expressed in dimensionless form as follows:

$$\frac{\mathrm{d}\gamma_n}{\mathrm{d}\tau} = \upsilon_n, \tag{5}$$

$$\frac{\mathrm{d}\upsilon_n}{\mathrm{d}\tau} = \frac{1}{\beta_{Cn}}[i - g_n\upsilon_n - \sin(\gamma_n) - i_{\mathrm{sn}} - g_n\alpha_n(\upsilon_1 + \upsilon_2)], \tag{6}$$

$$\frac{\mathrm{d}i_{\mathrm{sn}}}{\mathrm{d}\tau} = \frac{1}{\beta_{Ln}}(\upsilon_n - i_{\mathrm{sn}}). \tag{7}$$

Here, the normalized time $\tau = \omega_{\mathrm{c}1}t$ with $\omega_{c1} = (2eI_{\mathrm{c}1}R_{\mathrm{s}1})/\hbar$. All voltages are normalized to $I_{c1}R_{s1}$ and all currents normalized to I_{c1}, with taking $I_{c1} = I_{c2}$. The normalized junction voltage: $\upsilon_n = V_n/I_{c1}R_{s1}$. The normalized external dc bias current: $i = I_{\mathrm{dc}}/I_{c1}$. The normalized shunt current: $i_{\mathrm{sn}} = I_{\mathrm{sn}}/I_{c1}$. Other dimensionless parameters are as follows:

$$\beta_{Cn} = 2eI_{\mathrm{cn}}R_{\mathrm{sn}}^2C_n/\hbar,$$
$$\beta_{Ln} = 2eI_{\mathrm{cn}}L_n/\hbar,$$
$$g_n = R_{\mathrm{sn}}/R_{V1},$$

and $\alpha = \alpha_1 = \alpha_2 = R_{V1}/R = R_{V2}/R$ is used to denote the coupling intensity between two Josephson junctions (JJs) used in the array.

3. Generation of hyperchaos in the RCLSJJ array

To investigate hyperchaotic generation in the RCLSJJ array, we solve Eqs. (5)–(7) numerically. In the present work, the differential equations are solved using the fourth-order Runge–Kutta method with a fixed step $\Delta\tau = 0.01$ and total steps $N_{\mathrm{step}} = 10^5$, the Lyapunov exponents are computed using the algorithms presented by Wolf[27] and the voltage bifurcation diagrams are plotted by recording the local maxima in the voltage time series.[28]

To illustrate the process of hyperchaotic generation, firstly, we consider case 1 in which two RCLSJJs are in chaotic state before they are coupled and used in the array. The parameter values we used here are obtained from Refs. [3] and [5] at temperature $T = 7.60$ K and as follows: $\beta_C = \beta_{C1} = \beta_{C2} = 0.707$, $\beta_L = \beta_{L1} = \beta_{L2} = 2.68$, $g = g_1 = g_2 = 0.0478$, and $i = 1.2$. The initial values are $\gamma_1^0 = 0.2$, $\upsilon_1^0 = 2.5$, $i_{\mathrm{s}1}^0 = 0.2$, $\gamma_2^0 = 0.1$, $\upsilon_2^0 = 2.0$, and $i_{\mathrm{s}2}^0 = 0.1$. The numerical results of Eqs. (5)–(7), i.e. the bifurcation diagrams and Lyapunov exponents λ_1 and λ_2, are shown in Fig. 2. At the same time, we also compute other Lyapunov exponents $\lambda_3 \sim \lambda_6$ and find that they are negative in the selected range of parameters, thus they are not presented in Fig. 2.

From Figs. 2(a) and 2(b), one can see that for $0.200 \le \alpha \le 1.119$ the array and two JJs used in this array are in chaotic states which are occasionally interrupted by periodic windows; for $1.119 < \alpha \le 1.300$ two JJs are in the 2-period (2P) state and the array is in 1-period (1P) state. Here, near $\alpha = 1.119$, with α value reducing, the array and two JJs enter into chaotic states through intermittency routes. From Fig. 2(c), one can find that for $0.20 \le \alpha \le 0.36$ Lyapunov exponents λ_1 and λ_2 are both positive,

thus this array system is in a hyperchaotic state; for $0.36 < \alpha \leq 0.63$ Lyapunov exponent λ_1 is positive except 28 regions, i.e., $0.488 < \alpha < 0.504$, $0.547 < \alpha < 0.562$, $0.578 < \alpha < 0.589$, and near $\alpha = 0.365$, 0.378, 0.386, 0.394, 0.400, 0.408; 0.423, 0.427, 0.432, 0.440, 0.448, 0.455, $\alpha = 0.470$, 0.475, 0.483, 0.517, 0.524, 0.529, 0.534, 0.539, 0.568, 0.595, 0.602, 0.607, and $\alpha = 0.616$, where the λ_1 is near zero and λ_2 is negative, thus this array system is in a chaotic state and occasionally interrupted by these 28 periodic windows, which also can be seen by locally enlarging Figs. 2(a) and 2(b) [corresponding local enlarged figures are not presented in this paper]; for $0.630 < \alpha \leq 1.105$, λ_1 is positive and λ_2 is near zero, thus this array system is in chaotic state; for $1.105 < \alpha < 1.109$ and $1.115 < \alpha \leq 1.119$, λ_1 is positive and λ_2 is negative, thus this array system is in chaotic states; for $1.109 \leq \alpha \leq 1.115$ and $1.119 < \alpha \leq 1.300$, λ_1 is near zero and λ_2 is negative, thus this array system and two JJs are in periodic states.

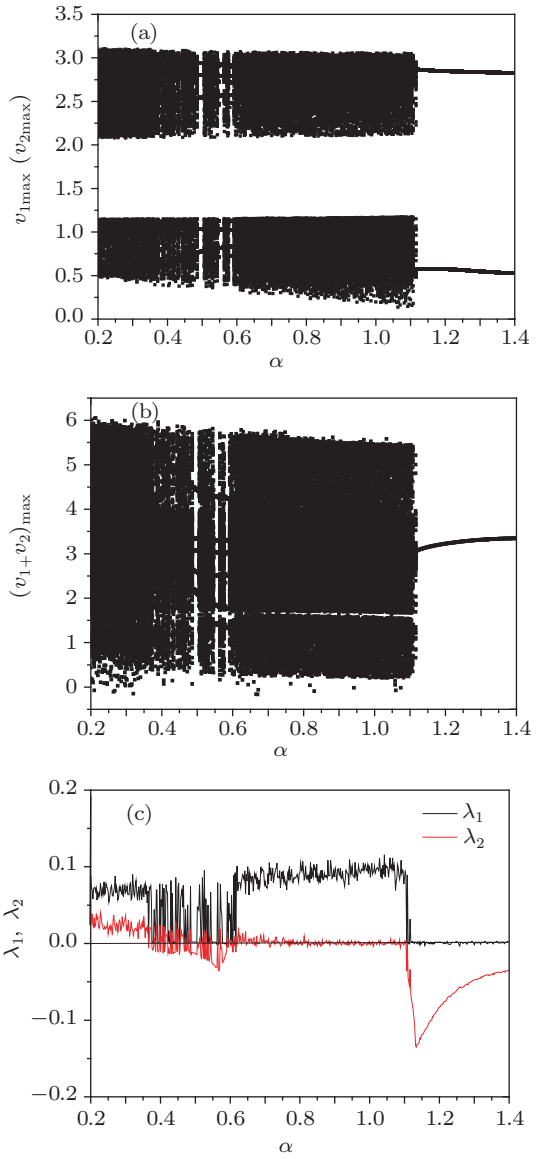


Fig. 2. (a) Bifurcation diagram of two junctions versus α; (b) the bifurcation diagram of the JJA versus α; (c) the Lyapunov exponents λ_1, λ_2 versus α.

Here, we compare the periodic motion behaviours in Figs. 2(a) and 2(b). In the range of $1.119 < \alpha \leq 1.300$, the relationship of the oscillation characteristics of two junctions and this array will be illustrated. Now $\alpha = 1.27$ is chosen, the corresponding time series of phase differences γ_1 and γ_2, and the time series of junction voltages v_1, v_2 and array output voltage $(v_1 + v_2)$ are shown in Figs. 3(a) and 3(b), respectively. From Fig. 3(a), one can see that two junctions are in the anti-phase case[29] in which two junctions have the same normalized oscillation period T but with staggered phases: $\gamma_1(\tau) = \gamma_2(\tau + (T/2))$. Thus, in Fig. 3(b), the junction voltages v_1 and v_2 undergo the same T periodic oscillation but the time interval of peak values of v_1 and v_2 is $T/2$, so the oscillation period of this array output voltage $(v_1 + v_2)$ is also $T/2$. Thus, for $1.119 < \alpha \leq 1.30$ both junctions are in 2P oscillation states and the array is in 1P oscillation states.

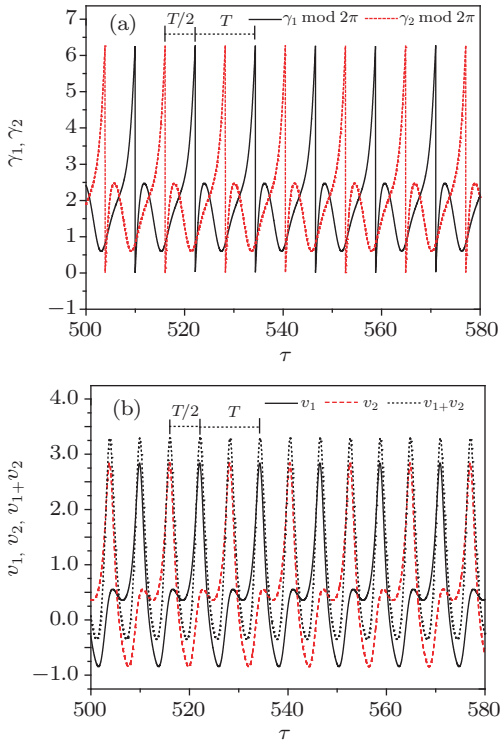


Fig. 3. (a) Time series of phase differences γ_1 and γ_2; (b) time series of voltages v_1, v_2, and $v_1 + v_2$.

Secondly, we consider case 2 in which two RCLSJJs are in periodic states before being coupled. According to Refs. [3] and [5], we take $\beta_L = \beta_{L1} =$

$\beta_{L2} = 2.5$, and other parametric values are the same as those in Fig. 2. The numerical results of Eqs. (5)–(7), i.e., the bifurcation diagrams and Lyapunov exponents λ_1 and λ_2 are shown in Fig. 4. Similarly, the other Lyapunov exponents $\lambda_3 \sim \lambda_6$ are negative in the selected range of parameters and are not presented in Fig. 4.

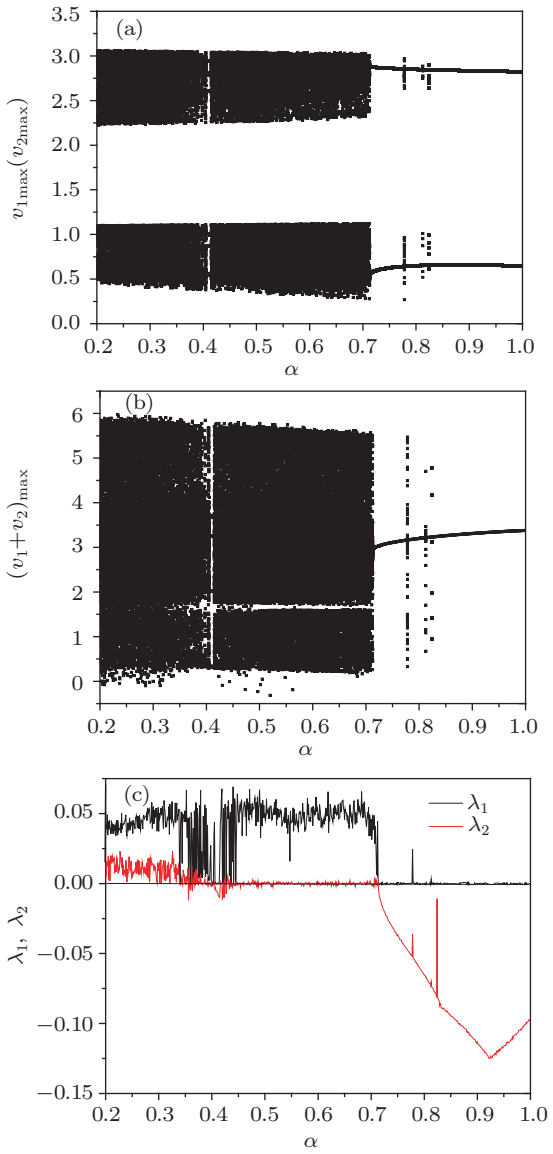


Fig. 4. (a) Bifurcation diagrams of two junctions versus α; (b) bifurcation diagram of JJA versus α; (c) Lyapunov exponents λ_1, λ_2 versus α.

From Figs. 4(a) and 4(b), one can see that for $0.20 \leq \alpha < 0.713$ and $0.777 \leq \alpha \leq 0.813$, the array and two JJs are in chaotic states, which are occasionally interrupted by periodic windows. For $0.713 \leq \alpha < 0.777$ and $0.813 < \alpha \leq 1.00$ two JJs are in 2P states, and the array is in 1P state. In the right end of bifurcation diagrams, with α value decreasing, the array and two JJs enter into chaotic states through intermittency routes. From Fig. 4(c), one can find that for $0.20 \leq \alpha < 0.34$ Lyapunov exponents λ_1 and λ_2 are both positive, thus this array system is in the hyperchaos state; for $0.340 \leq \alpha \leq 0.445$ the λ_1 is positive except 16 regions, i.e., $0.406 < \alpha < 0.414$, $0.399 < \alpha < 0.403$ and near $\alpha = 0.340$, 0.356, 0.360, 0.363, 0.366, 0.368, 0.372, 0.375, 0.420, 0.423, 0.427, $\alpha = 0.436$, 0.441, and $\alpha = 0.445$, where λ_1 is near zero or negative and λ_2 is negative or near zero, thus this array system is in chaos state occasionally interrupted by these 16 periodic windows, which can also be observed by locally enlarging Figs. 4(a) and 4(b) [corresponding local enlarged figures are not presented in this paper]. For $0.445 < \alpha < 0.713$, the λ_1 is positive and λ_2 is near zero, thus this array system is in a chaotic state. For $0.713 \leq \alpha < 0.777$, $0.779 < \alpha < 0.813$, and $0.813 < \alpha \leq 1.00$, λ_1 is near zero and λ_2 is negative, thus this array system and two JJs are in periodic states. For $0.777 \leq \alpha \leq 0.779$ and near $\alpha = 0.813$, λ_1 is positive and λ_2 is negative, thus this array system and two JJs are in chaos states.

Similarly, to illustrate the relationship of periodic oscillations of two junctions and this array, according to Figs. 4(a) and 4(b), $\alpha = 1.00$ is chosen. The corresponding time series of phase differences γ_1 and γ_2, as well as junction voltages v_1, v_2, and the array output voltage $v_1 + v_2$ can be obtained by numerically solving Eqs. (5)–(7), and they are similar to Figs. 3(a) and 3(b). Thus two junctions are also in anti-phase state with $\gamma_1(\tau) = \gamma_2(\tau + (T/2))$

To further show dynamical behaviours of different states in the array, according to Fig. 2(c), $\alpha = 0.2$, 1.0, 1.27 are chosen, the corresponding attractors, time series, and power spectra are presented in Fig. 5, where figures 5(a1)–5(a3) show that this array is in hyperchaotic state; figures 5(b1)–5(b3) show that this array is in chaotic state; Figs. 5(c1)–5(c3) show that this array is in 1P state.

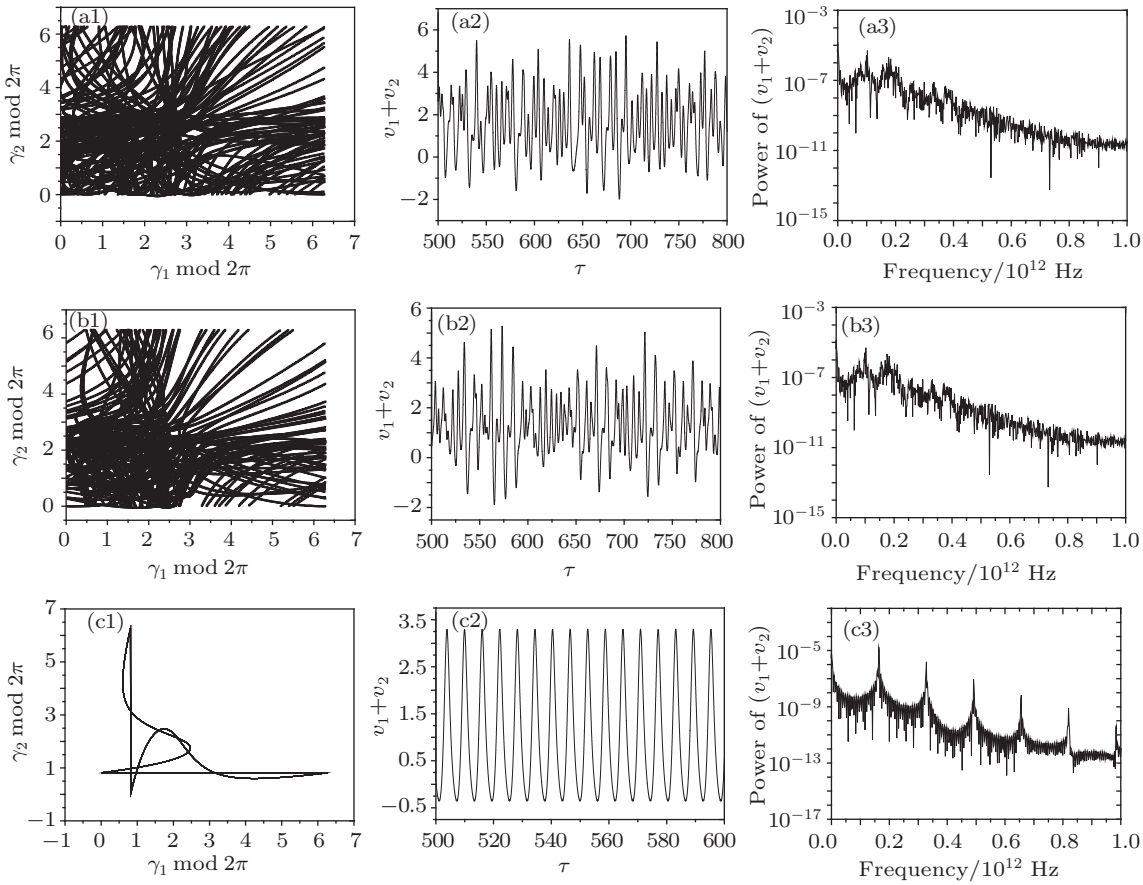


Fig. 5. Attractors on plane γ_1–γ_2, time series of all voltage $(v_1 + v_2)$ and power spectra of all voltage $(v_1 + v_2)$ in different α values. Panels (a1)–(a3) for $\alpha = 0.2$, (b1)–(b3) for $\alpha = 1.0$, and (c1)–(c3) for $\alpha = 1.27$.

4. Controlling hyperchaos in the RCLSJJ array

Here we propose a scheme for controlling hyperchaos in the RCLSJJ array by adjusting the external bias dc current i based on the theory of nonfeedback control of chaos.[30] To illustrate the process of controlling hyperchaos in this scheme, firstly let this array remain in the hyperchaotic state as shown in Figs. 5(a1)–5(a3). Secondly, numerical simulations are carried out by solving Eqs. (5)–(7) by using i as a control parameter. The bifurcation diagram and Lyapunov exponents are presented in Fig. 6, where one can see that exponent λ_2 is near zero or negative in the selected range of parameters, thus hyperchaotic states disappear; for $1.012 < i \leq 1.100$ the maximum Lyapunov exponent λ_1 is near zero, thus this array is in periodic state.

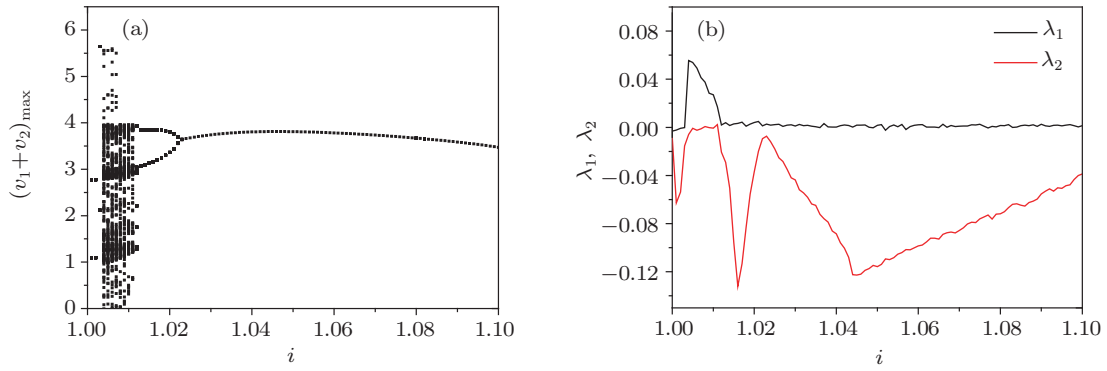


Fig. 6. (a) Bifurcation diagram of the array versus i; (b) Lyapunov exponents λ_1, λ_2 versus i.

To further clarify that the array can be controlled into different period states, according to Fig. 6, $i = 1.02$ and $i = 1.05$ are chosen. The corresponding attractors, time series and power spectra are shown in Fig. 7, where Figs. 7(a1)–7(a3) and 7(b1)–7(b3) denote that this array is in 2P state and 1P state, respectively. It is remarkable that the array is in hyperchaotic state as shown in Figs. 5(a1)–5(a3) before being controlled, thus the hyperchaotic state in this array can be controlled into different stable period states, such as 2P and 1P states as shown in Figs. 7(a) and 7(b), respectively.

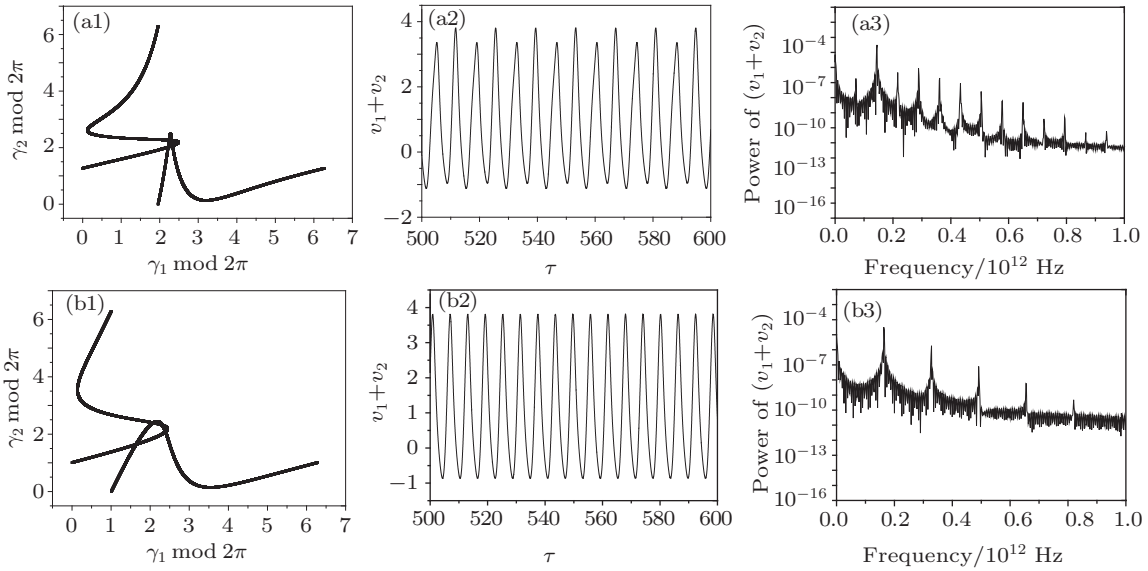


Fig. 7. Attractors on plane γ_1–γ_2, time series of all voltage $(v_1 + v_2)$, and power spectra of all voltage $(v_1 + v_2)$ in different i values; panels (a1)–(a3) for $i = 1.02$, and the array in 2P state; panels (b1)–(b3) for $i = 1.05$, and the array in 1P state.

5. Conclusion

In this paper we studied the dynamical characteristics in an array composed of two RCLSJJs and a shunted resistor by using bifurcation diagrams and Lyapunov exponents. Numerical simulations demonstrated that hyperchaotic, chaotic and periodic states can coexist in this array by changing coupling intensity, no matter whether two junctions are in chaotic states in advance or not. Moreover a scheme for controlling the hyperchaotic state in this array is presented by adjusting the external bias dc current. Numerical results confirmed that this scheme can be used to effectively control the hyperchaotic state in this array into stable periodic states and the different periodic states with different period numbers can be obtained by choosing appropriate intensity of the external dc bias current. Here the hyperchaos state in the JJA is reported for the first time. These results are useful for fabricating and applying a JJA composed of RCLSJJs.

References

[1] Benz S P and Buuroughs C 1991 *Appl. Phys. Lett.* **58** 2162
[2] Whan C B and Lobb C J 1996 *Phys. Rev.* E **53** 405
[3] Whan C B, Lobb C J and Forrester M G 1995 *J. Appl. Phys.* **77** 382
[4] Cawthorne A B, Whan C B and Lobb C J 1997 *IEEE Trans. Appl. Supercond.* **7** 2359
[5] Whan C B and Lobb C J 1996 *Phys. Rev.* E 53 405
[6] Cawthorne A B, Whan C B and Lobb C J 1998 *J. Appl. Phys.* **84** 1126
[7] Cawthorne A B, Barbara P, Shitov S V, Lobb C J, Wiesenfeld K and Zangwill A 1999 *Phys. Rev.* B **60** 7575
[8] Yang X S and Li Q 2006 *Chaos, Solitons and Fractals* **27** 25
[9] Dana S K, Roy P K, Sethia G C, Sen A and Sengupta D C 2006 *IEEE Proc. Circ. Dev. Syst.* **153** 453
[10] Ucar A, Lonngren K E and Bai E W 2007 *Chaos, Solitons and Fractals* **31** 105
[11] Feng Y L and Shen K 2008 *Chin. Phys.* B **17** 111
[12] Feng Y L, Zhang X H, Jiang Z G and Shen K 2010 *Int. J. Mod. Phys.* B **24** 5675
[13] Feng Y L and Shen K 2008 *Eur. Phys. J.* B **61** 105
[14] Feng Y L and Shen K 2008 *Chin. Phys.* B **17** 550
[15] Feng Y L, Zhang X H, Jiang Z G and Shen K 2009 *Int. J. Mod. Phys.* B **23** 3601
[16] Feng Y L and Shen K 2010 *Chin. J. Phys.* **48** 316

[17] Basler M, Krech W and Platov K Y 1995 *Phys. Rev.* B **52** 7504
[18] Hassel J, Gronberg L, Helisto P and Seppa H 2006 *Appl. Phys. Lett.* **89** 072503
[19] Grib A N, Seidel P and Scherbel J 2001 *Phys. Rev.* B **65** 094508
[20] Bhagavatula R, Ebner C and Jayaprakash C 1994 *Phys. Rev.* B **50** 9376
[21] Chernikov A A and Schmidt G 1994 *Phys. Rev.* E **50** 3436
[22] Zhou T G, Mao J, Liu T S, Lai Y and Yan S L 2009 *Chin. Phys. Lett.* **26** 077401
[23] Klushin A M, He M, Yan S L and Klein N 2006 *Appl. Phys. Lett.* **89** 232505
[24] Zhou T G, Yan S L, Zou X, Li S, Ji L and Zhao X J 2006 *Chin. Phys. Lett.* **23** 1935
[25] Zhang S H and Shen K 2003 *Chin. Phys.* **12** 149
[26] Feng X Q, Yao Z H, Tian Z L and Han X Y 2010 *Acta Phys. Sin.* **59** 8414 (in Chinese)
[27] Wolf A, Swift J B, Swinney H L and Vastano J A 1985 *Physica* D **16** 285
[28] Sprott J C 1997 *Phys. Lett.* A **228** 271
[29] Hadley P and Beasley M R 1987 *Appl. Phys. Lett.* **50** 621
[30] Hu G, Xiao J H and Zheng Z G 2000 *Chaos Control* (Shanghai: Shanghai Scientific and Technological Education Publishing House) pp. 54–57